Tribology International, Volume 38, Issue 5, May 2005, Pages 469-480.

Identification of the Acoustic Emission source during a comparative study on diagnosis of a spur gearbox

Chee Keong Tan and David Mba

School of Engineering, Cranfield University, Bedfordshire. MK43 0AL, UK

Tel +44 (0) 1234-754681, Fax: +44 (0) 1234-751566.

E-mail: c.k.tan@cranfield.ac.uk and d.mba@cranfield.ac.uk

Abstract

Condition monitoring of gears with vibration analysis is well established whilst the application of Acoustic Emission (AE) to gear defect diagnosis and monitoring is still in its infancy. This paper details results of an experimental programme to ascertain and validate the applicability of AE to seeded gear defect identification. Furthermore, comparisons are made to vibration diagnosis. As a direct consequence of the experimental programme, the relationship between temperature, oil film thickness and AE activity were investigated. It is shown that similar to the lubricant film thickness between non-conforming surfaces under isothermal conditions, AE activity is not influenced by load. Limitations of applying AE to seeded defect identification are presented and it is concluded that the source of AE activity is attributed to asperity contact.

Keyword: Acoustic Emission, asperity contact**,** condition monitoring, gear defect diagnosis, lubricant film thickness, rolling friction, sliding friction.

1. Introduction

The application of Acoustic Emission (AE) to static structures is well documented [1]. However, the application of AE to fault diagnosis of rotating machines is in its infancy [2–10]. The use of vibration analysis to gear fault diagnosis and monitoring has been widely investigated and its application in industry is well established [11-13]. This is particularly reflected in the aviation industry where the helicopter engine, transmission systems, drive trains and rotor systems have been fitted with vibration systems for component health and monitoring.

Drosjact et al [14] attempted to establish the actual physical mechanism that caused vibration change in the gear defect frequencies. Drosjact et al postulated that changes in tooth thickness due to presence of pits caused modifications in the Hertzian compliance. Furthermore, it was suggested that pitting will cause instantaneous changes in Hertzian stiffness which generate a Hertzian impact due to the sudden velocity differences between the pinion and wheel. In addition, micro pitting was also identified as a source of increased vibrations. Micro pitting is related to the initiation of other failure modes such as pitting, scuffing, and flank initiated bending failures.

Research publications in the application of AE to gear fault detection and monitoring are limited. This paper explores the applicability of AE to gear defect diagnosis. Furthermore, it explores the source of AE activity from the gearbox.

2. Acoustic Emission

Acoustic Emission is defined as the transient elastic wave generation due to a rapid release of strain energy within or on the surface of a material. These waves are detected at the surface of the body by a suitable sensor. The principal advantage of AE comes from its high sensitivity. Since AE is produced at a microscopic level, it is more sensitive to detection of loss of mechanical integrity as compared to the well established vibration monitoring technique. The main disadvantage of using AE is attenuation experienced over distances and particularly across interfaces.

3. Literature Reviews

Toutountzakis et al [6] presented some interesting observations on AE activity due to misalignment and natural pitting and concluded that the AE technique was a viable technique for monitoring gear deterioration. Tandon et al. [15] concluded that the AE parameters increased with increased defect size (diameter of pit) and load. Tandon also revealed that the AE technique was able to detect smaller defects in comparison to vibration measurements.

Singh et al [16, 17] noted that AE could provide earlier detection over vibration monitoring for pitting of gears, excluding extremely high gear speeds or unloaded gear conditions. Furthermore, it was commented that AE could detect crack initiation and growth, while the accelerometer could only detect the crack growth at a later stage of the crack growth process. The final experiment performed by Singh et al involved an assessment of the transmissibility of AE signal within a gearbox. It was concluded that the attenuation across the gearbox was an accumulation of losses across each individual interface within the transmission path. Sentoku [18] correlated tooth surface damage such as pitting to AE whilst Siores et al [19] concluded that the AE results could be correlated to various defect conditions.

The papers reviewed have illustrated the potential of AE becoming a useful diagnostic tool in condition monitoring of gears.

4. Experimental set-up

4.1 Gearbox

The test-rig employed for this investigation consisted of two identical oil-bath lubricated gearboxes, connected in a back-to-back arrangement, see figure 1. The 49 and 65 teeth gear sets were made of 045M15 steel without heat treatment. The gears have a pressure angle of 20°, module of 3 mm and surface roughness between 2-3 μm (before running-in). Each gearbox had four identical bearings. The method of applying torque was a simple mechanism that allowed a pair of coupling flanges to be rotated relative to each other, and locked in position. This effectively locks the torque within the gearboxes

ensuring that the motor used to drive the test rig only overcome power losses associated with the meshing gears. It must be noted that the 0 Nm condition is not literally '0 Nm'. There will exist a light load at this condition due to the bearing friction and losses/resistance associated with the rubber seals, gear churning and windage. If a true '0 Nm' condition was obtainable, the gear would run in a non-linear manner. The motors used to drive the gearbox were single speed motors (1.1 kw and 0.55 kw) providing a rotational speed of 745 rpm and 1460 rpm respectively. For these experimental investigations, five torque loadings were used; 0 Nm, 55 Nm, 110Nm 183 Nm and 220 Nm.

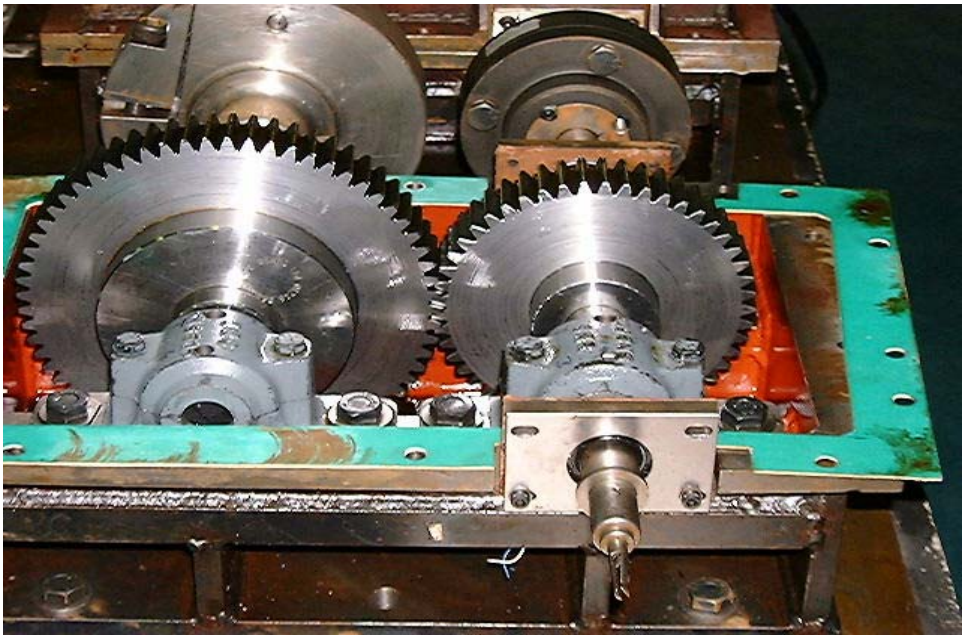

Figure 1 Test-rig gearbox arrangement.

4.2 Data Acquisition

The AE sensors used for this experiment were wide band type sensors with a relative flat response between 100 kHz and 1 MHz (WD model, 'Physical Acoustics Corporation'). An AE sensor was placed on the pinion (49 teeth), see figure 2. The cable connecting the pinion sensor was fed into the pinion shaft to the pre-amplifier via a slip ring. This arrangement allowed the AE sensor to be placed as close as possible to the gear teeth. Both sensors were held in place with mechanical fixtures. An 'IDM Electronics Ltd' manufactured PH-12 slip ring was employed. The slip ring used sliver contact and could accommodate a maximum of 12 channels. The cooling air pressure for the slip ring was 1400 kg/mm^2. Pre-amplification was set at 40dB. The signal output from the pre-amplifier was connected (i.e. via BNC/coaxial cable) directly to a commercial data acquisition card. The data acquisition card could provide 10 MHz sampling rate and incorporated 16-bit precision giving a dynamic range of more than 85 dB. Prior to the analog-to-digital converter (ADC), the card employed anti-aliasing filters that can be controlled directly in software. A K-type (Chromel-Alumel) thermal couple, rated from -200^0C to 1378^0C, was employed to measure the oil temperature for computation of oil film thickness. The oil bath temperature was measured through an opening on top of the gearbox casing using the specified thermal couple probe. This position for acquiring oil temperatures was adjacent to the gear mesh position as this was the closest position the authors could get access to.

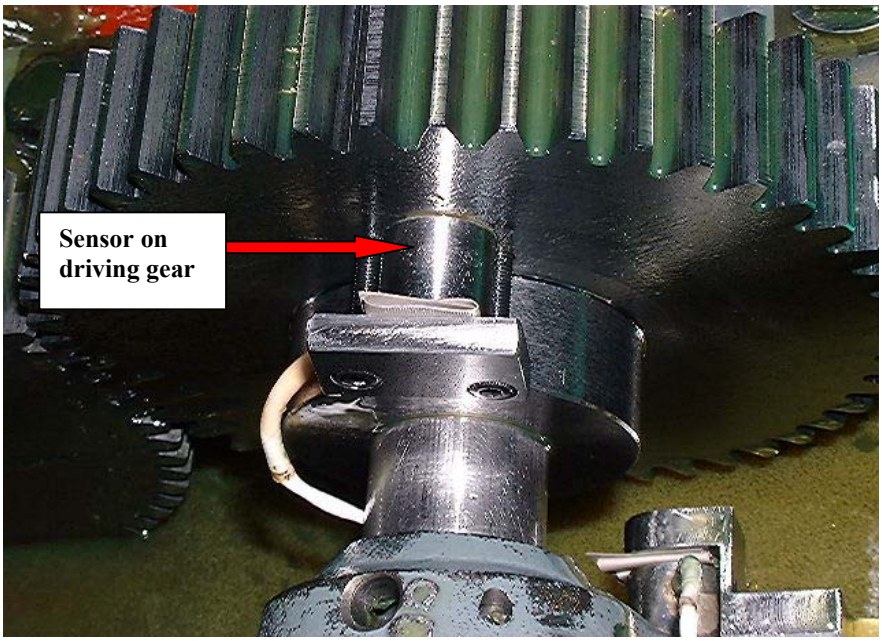

Figure 2 AE sensor located on the pinion.

The accelerometer (see figure 3) used for vibration measurement in this experiment was resonant type sensor with a flat frequency response between 10 Hz and 8000 Hz (Model 236 Isobase accelerometer, 'Endevco Dynamic Instrument Division'). The accelerometer was mounted on the base of the pinion bearing casing to capture vibration data of the gearbox. The charge amplifier employed was a single channel PE amplifier (Endevco Dynamic Instrument Division, Model 2721B). The accelerometer was connected to a charge amplifier, and the signal output from the pre-amplifier was fed to a commercial data acquisition card. Energy, r.m.s and frequency domain information were computed from the raw time-domain data. A 1V peak from the pre-amplifier corresponded to 1g. This was calibrated using a calibration table from Endevco.

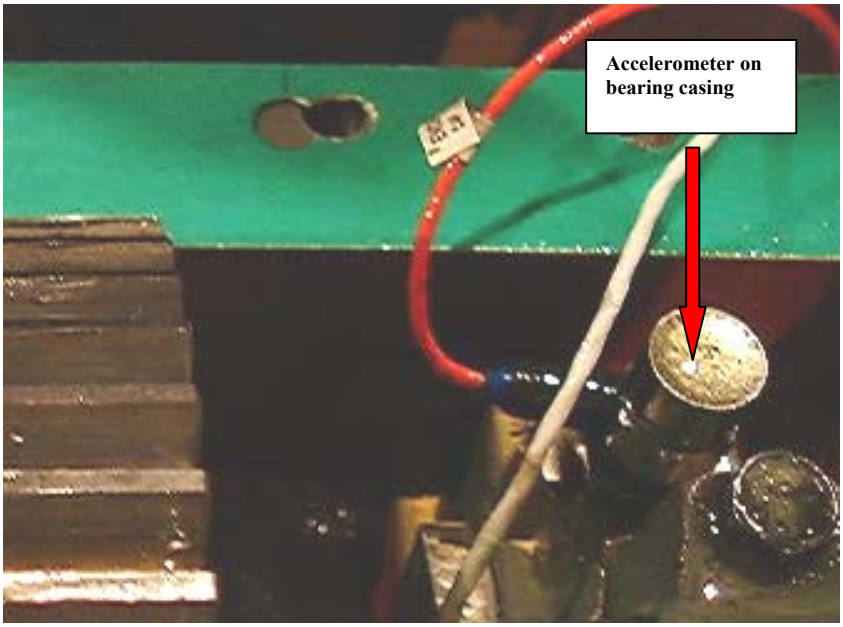

Figure 3 Accelerometer located on bearing casing.

5. Test procedure

Prior to the start of the experiment the gearbox was ran for 15 hours. Following this a large addendum defect (extended from the pitch-line) measuring 12 mm along the face width and 3 mm from the pitch-line to the gear tip was seeded on one of the pinion tooth surface, see figure 4. A total of six experimental combinations were undertaken: two speed and three load conditions. For each test condition, the gearbox ran from a cold start for several hours until the oil temperature reached equilibrium, i.e. it reached a temperature that did not change as a function of running time. Equilibrium was established when oil temperature varied by less than 0.2^0C for a period of one hour. The oil temperatures and vibration data were taken at 15 minute intervals throughout the duration of the test whilst AE r.m.s. and energy values were monitored continuously (see

section 9.1). AE time signatures were acquired for each test condition after 30 minutes from the start. For analysis of AE data obtained from these experiments, r.m.s and energy were employed to provide a comparison to other published work and because of the simplicity and proven robustness of these parameters for machine health diagnosis.

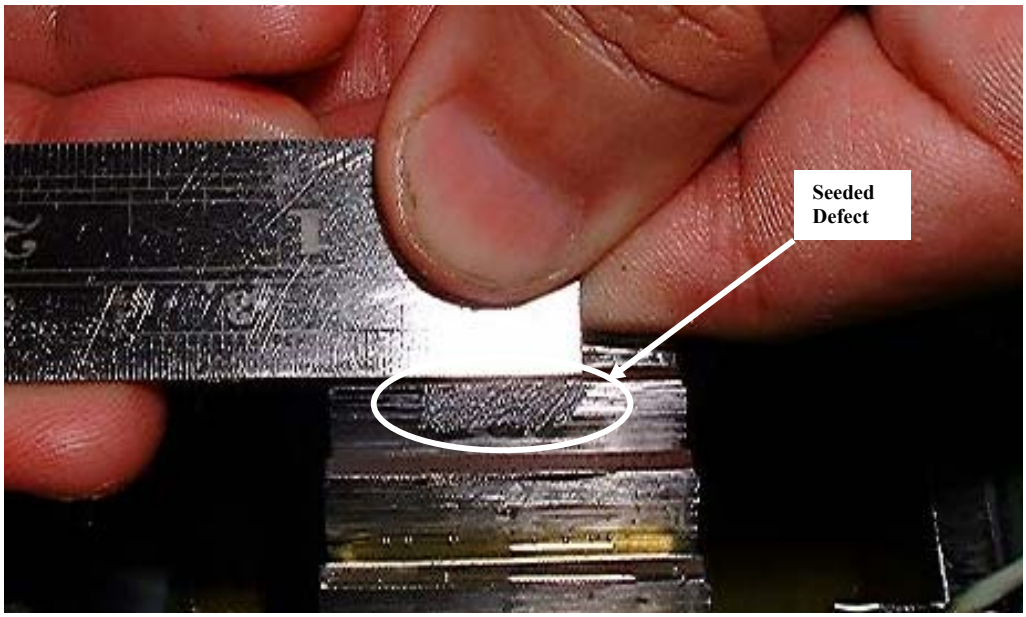

Figure 4 Seeded large addendum defect.

6. Results of operational background noise

Figure 5 displays a typical AE signature with corresponding frequency spectrum associated with operational background noise. Background noise is defined as the operational condition of the machine prior to seeding the defect. It clearly shows 16 meshing gear teeth. The frequency range of the AE signals associated with these tests ranged from 70 kHz to 350 kHz. Figures 6 and 7 illustrate the time domain signatures for

the load and speed cases considered with the simulated defect. The gear mesh frequency can also be calculated from the time domain AE signal by calculating the rate of AE bursts, though this is only clearly evident at 745 rpm. At 1460 rpm, it is more difficult to separate the AE transients associated with the gear mesh. This is primarily because the authors could not increase the sampling rate of the acquisition beyond 10 MHz.

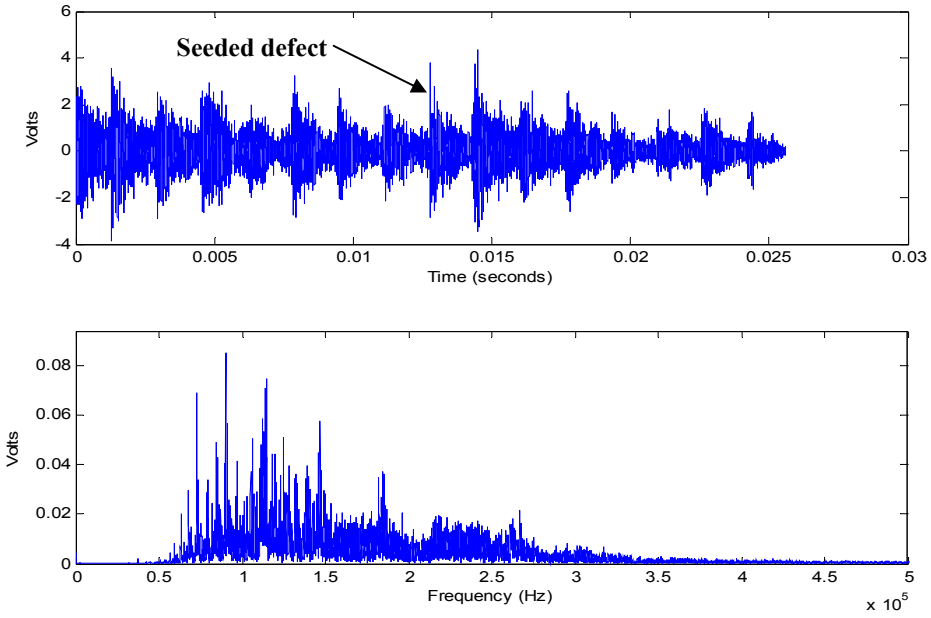

Figure 5 **Time and frequency domain of an AE signature showing clearly the AE transient response associated with gear meshing of 16 teeth for the rotational speed of 745 rpm; load 110 Nm.**

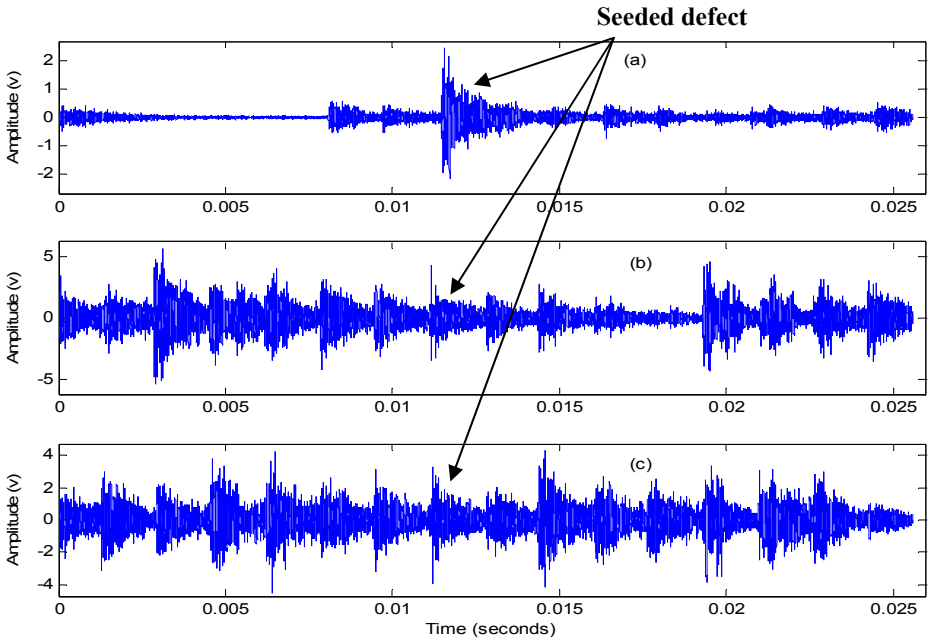

Figure 6 **Raw AE signal for large addendum defect for (a) no load, (b) 55 Nm load and (c) 110 Nm load at 745 rpm.**

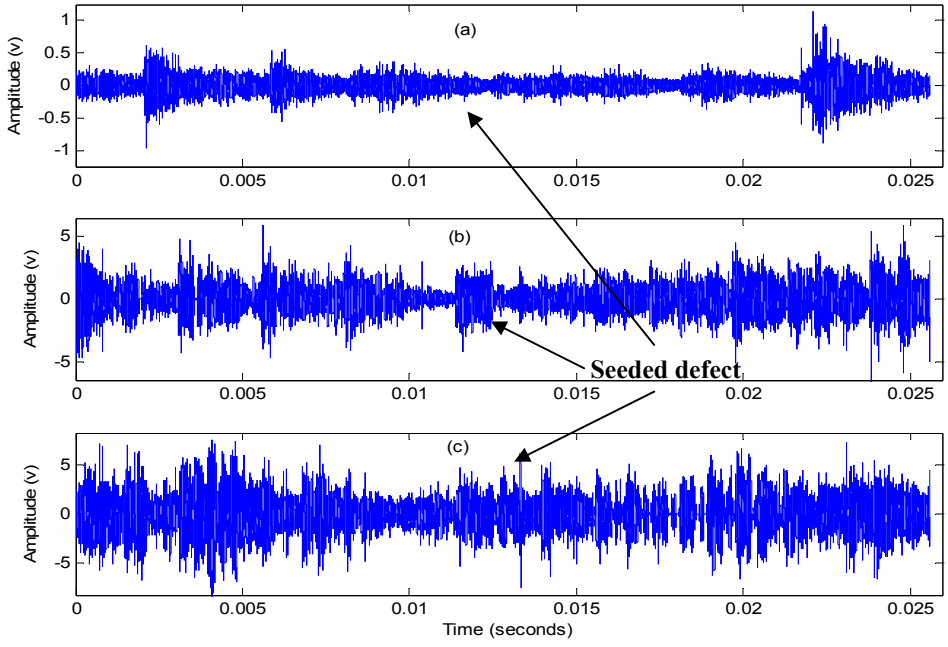

Figure 7 **Raw AE signal for large addendum defect for (a) no load, (b) 55 Nm load and (c) 110 Nm load at 1460 rpm.**

7. AE fault identification capability

For the rotational speeds of 745 and 1460 rpm, the recorded AE time waveform was split into regions representing 2-teeth and 1-tooth. Figure 8 illustrates the case for 2-teeth regions at 745 rpm. The r.m.s. value for each region was calculated for each data set. This was equivalent to '8' and '16' r.m.s values for 2-teeth and 1-tooth data sets respectively. A total of 50 data sets were acquired for each test condition and the r.m.s values presented were averaged for each region over all fifty data sets. The averaging could be accomplished due to the optical triggering system employed ensuring that the acquisition system always started at the same rotational position of the gears. It was thought that this method of grouping the data would enhance the possibilities of detecting the seeded defect particularly as the defect had been seeded in the centre of the acquisition window, see figure 8.

For the seeded defect simulation at 745 rpm, the r.m.s. values remained random for the three loading conditions, see figure 9. The centre region '4', where the seeded defect was introduced, did not exhibit the highest r.m.s. value as expected. The same observations were made for the rotational speed of 1460 rpm, the highest r.m.s. values did not happened in the seeded fault region of region '8', see figure 10.

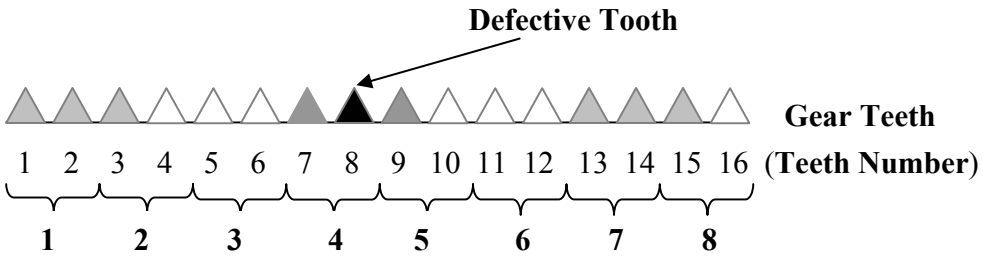

Figure 8 Sectioning of gear teeth for analysis.

Similar observations were noted using the single-tooth group, the r.m.s. value at the seeded fault tooth, regions '8' and '15' (based on a single tooth demarcation for 745 and 1460 rpm respectively), were not the highest values. These results revealed that this technique was unsuccessful for defect identification. Based on a normal distribution the variation in AE r.m.s at the seeded defect location fell within one-standard deviation while all AE r.m.s values were within two-standard deviations. The results would have been conclusive had the r.m.s. level for the defective tooth being higher than other regions within the acquisition window. For the same test condition, AE energy exhibited similar observations.

Examples of the raw AE signals from defect conditions are displayed in figures 6 and 7. This shows the non-consistent observation of AE burst in relation to the defect position. The largest amplitude burst of the AE signal did not always occur in the centre region of the window where the seed fault was located even though the defect was comparatively large. Hence, it was not possible to detect the seeded defect using the AE indicators of r.m.s. and energy. This contradicts the work of a few researchers [15, 16, 19] that claimed

AE indicators could clearly identify a simulated pit defect. It was interesting to note that in general, the r.m.s. values increased with increasing load conditions.

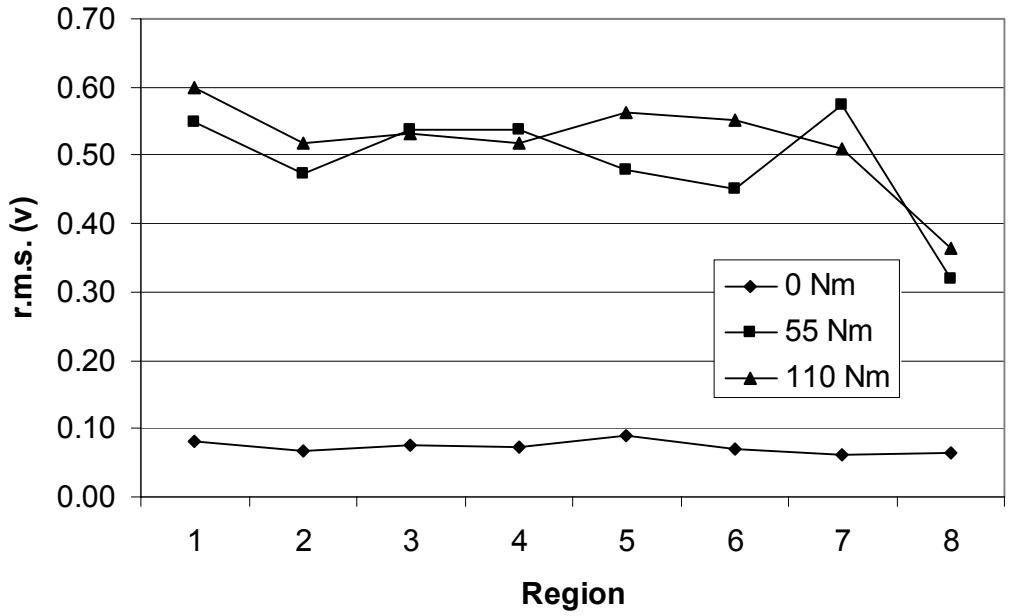

Figure 9 r.m.s against loads for 2-teeth analysis at 745 rpm. (8 regions)

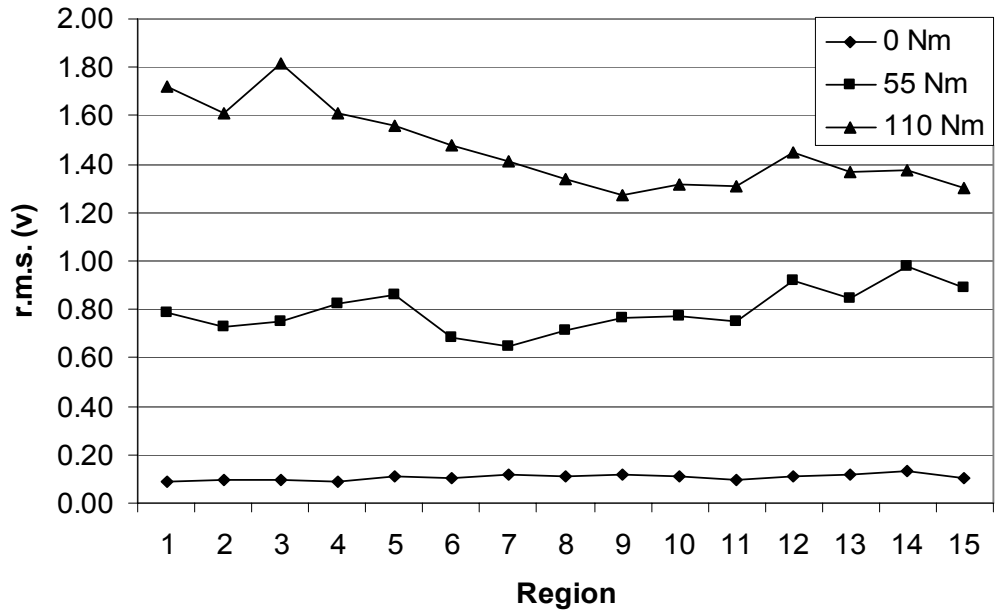

Figure 10 r.m.s against loads for 2-teeth analysis at 1460 rpm. (15 regions)

8. Vibration Analysis

From acquired vibration signatures, the r.m.s. and energy values were calculated, and vibration frequency spectrum investigated. A sampling rate of 8192 data points per second (8192 Hz) over duration of approximately five seconds (40000 data points), which is approximately equivalent to 61 and 119 revolutions, was employed for vibration data acquisition at rotational speeds of 745 and 1460 rpm respectively.

For the rotational speed of 745 rpm, all three load conditions exhibited similar frequency content; the highest peaks in the frequency domain occurred at the gear mesh frequency, 608 Hz, and sidebands were observed around this frequency (see figure 11). Harmonics of the gear mesh frequency were noted at 1200 Hz, 1800 Hz and 2400 Hz. The peak value at the gear mesh frequency increased from 0.5 to 1.0 g from no-load condition to 110 Nm. As side bands about the gear mesh frequency were observed, see figure 11, this was indicative of a defective tooth.

Vibration frequency spectra results at 1460 rpm are presented in figure 12. A unique observation was the wide band of frequency response ranging from 0 to 2600 Hz which was not present at the lower speed of 745 rpm (figure 11). Under no-load condition, the peak value at the gear mesh (GM) frequency of 1200 Hz was 0.03 g. The dominant frequencies in this spectrum were noted to be the sub-harmonics of the gear mesh frequency at 300, 400, 600 and 800 Hz (0.25, 0.33, 0.5 and 0.67 GM). When the load increased to 55 Nm, the dominant frequency was at 400 Hz (0.33 GM). Following an

increase in load to 110 Nm, the dominant frequency shifted back to the gear mesh frequency with a peak value of 0.2 g. It is also important to note the strong presence of the second harmonic gear mesh frequency at 2400 Hz. At this load side bands were observed about the gear mesh frequency, again evident of a defective tooth.

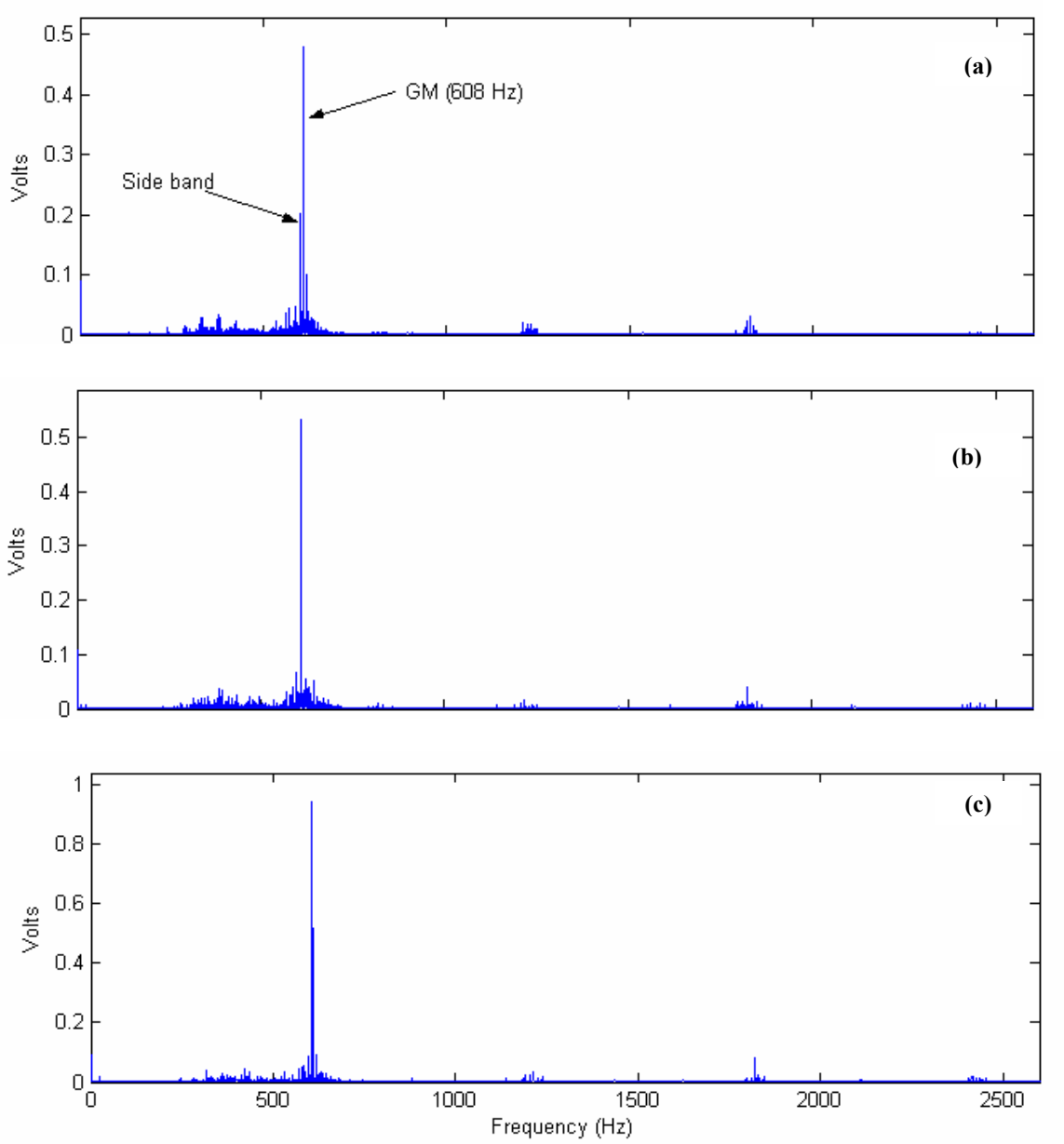

Figure 11 **Frequency spectra for (a) 0 Nm, (b) 55 Nm and (c) 110 Nm load conditions at 745 rpm.**

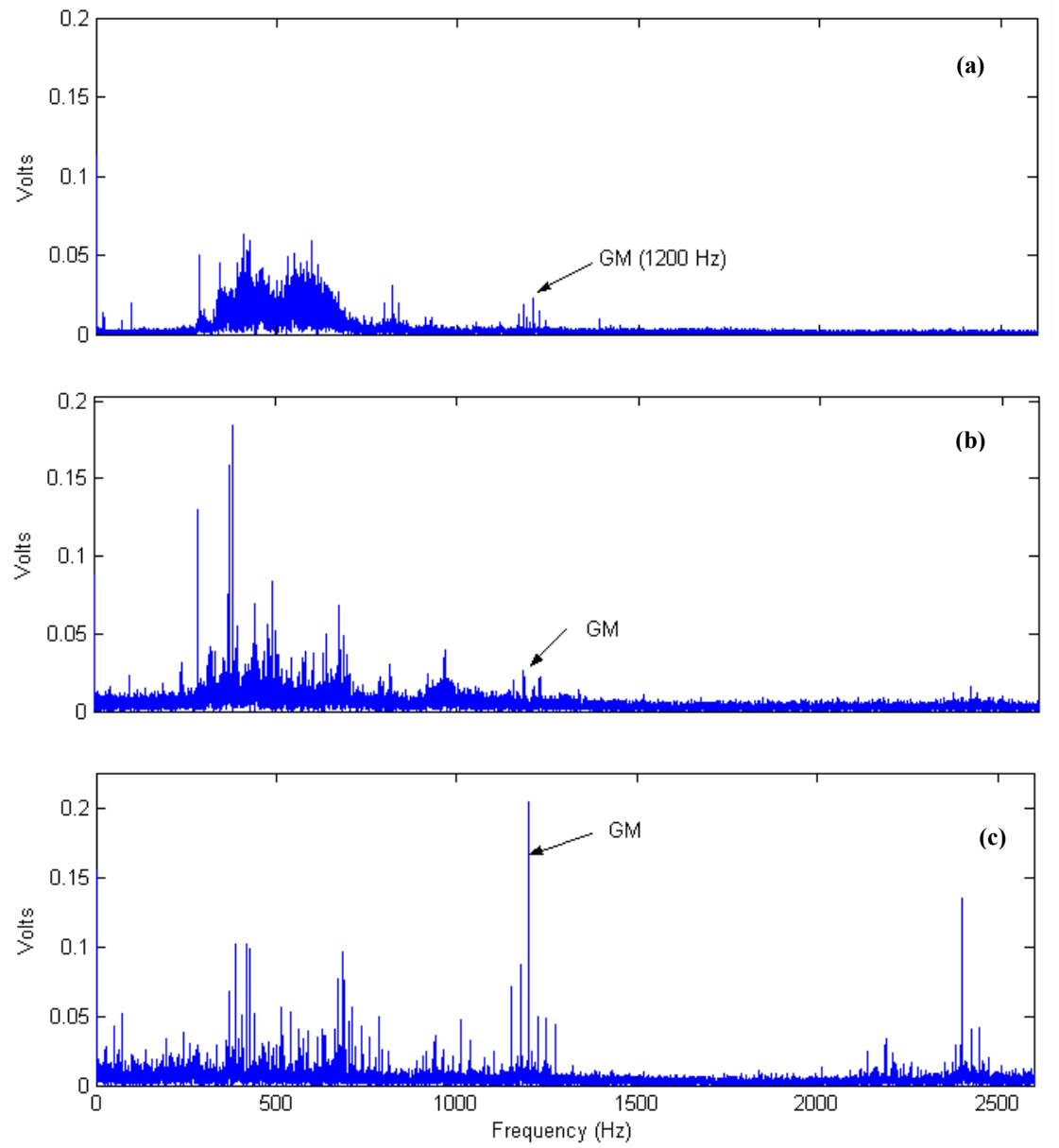

Figure 12 **Frequency spectra for (a) 0 Nm, (b) 55 Nm and (c) 110 Nm load conditions at 1460 rpm.**

Further investigations were undertaken to understand the unique frequency spectra at 1460 rpm. Gears are described as lightly loaded when applied load on the gear is not sufficiently high enough to maintain contact during meshing. The phenomenon usually

occurs due to light loads or high loads with large transmission errors (TE). Smith [21] stated that in general, the presence of strong harmonics at the tooth mesh frequency indicates loss of contact, and this condition is reinforced if the harmonics increase with reducing loads. From figure 12, the presence of strong harmonics at the gear mesh frequency was evident and the harmonics increased with a reduction in load. Hence, a lightly loaded condition was suspected to exist under certain conditions at 1460 rpm.

It was thought prudent to ascertain if the test gears could be considered as lightly loaded. Smith [21] details the procedure for determining such a condition. Assuming a Transmission Errors (TE) of 5 μm, which is typical for spur gears [21], the torques required to maintain the meshing teeth in contact was calculated at 43 Nm and 107 Nm for the pinion and gear respectively, both at a rotational speed of 1460 rpm. Hence, for the 55 Nm test condition, the applied load was lower than the required torque to maintain the meshing teeth in contact, 107 Nm, hence loss of contact was likely to occur, as confirmed earlier. For the 110 Nm test condition, the applied torque was marginally higher than the required torque of 107 Nm. Thus, it may be concluded that no contact loss occurred under this situation, which is evident from the differences in the frequency spectra between figure 12(c) and 12(b). Based on the same concept, the required torques for the gear teeth to remain in contact are also computed for the case of 745 rpm; 11 and 28 Nm for the pinion and gear respectively. With the minimum applied torque of 55 Nm, which is higher than the required torque of 28 Nm, the gears will not be lightly loaded.

Clearly, vibration analysis was capable of diagnosing the large seeded defect, however, this was not evident from analysis of AE data.

9. Oil Temperature and Film Thickness

To understand the limitations of the AE technique for defect identification further tests were undertaken. This involved measuring the oil temperature of the gearbox sump from a cold start to the operational oil temperature and calculating the oil film thickness between the gears. Results from the six test conditions were plotted to observe the effect of speed and load over the oil temperature and film thickness. For both speeds (745 and 1460 rpm), the operational oil temperatures increased with increased loads and speeds, see figures 13 to 15.

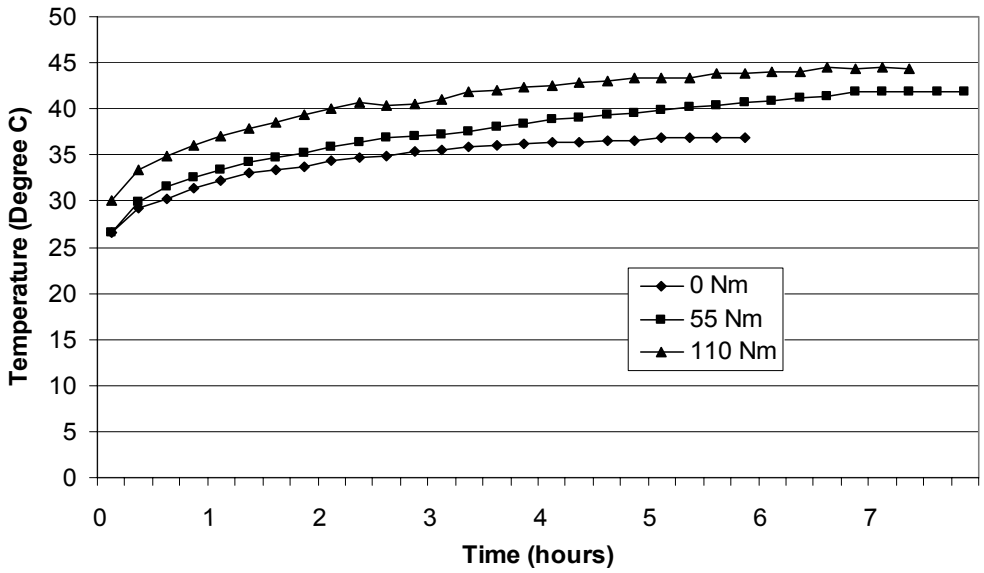

Figure 13 The effect of load on oil temperature for speed of 745 rpm.

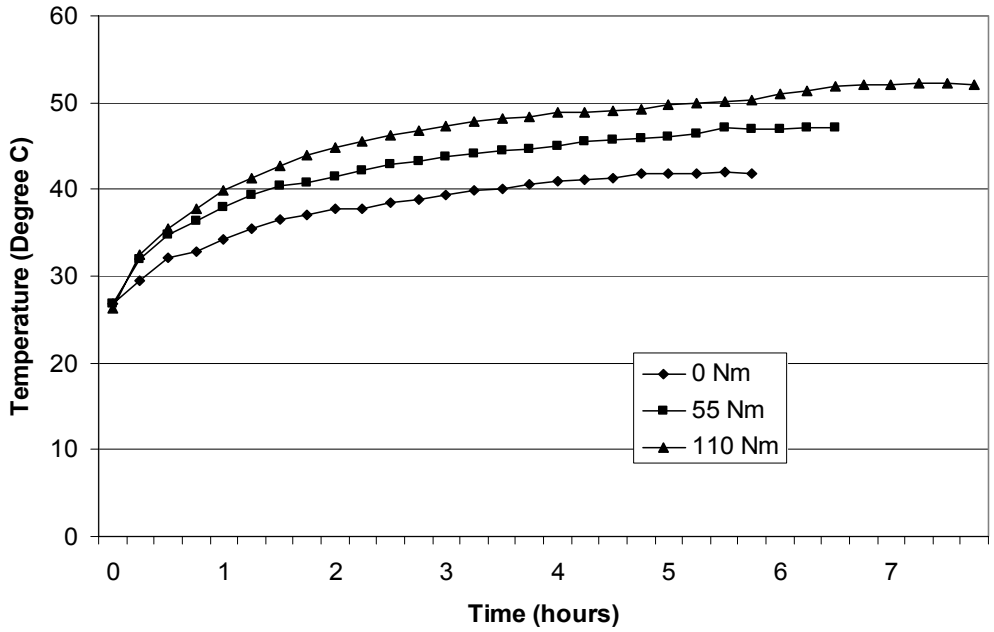

Figure 14 The effect of load on oil temperature for speed of 1460 rpm.

The oil film thickness, μm, [22] was calculated from equation (1)

$$h_{\min} = 0.325 \sin\phi (V_k d_1 V_1 \{\frac{r}{r+1}\})^{0.5} \quad (1)$$

Results of theoretical oil film thickness are presented in figures 16 and 17. Based on the surface finish of 1.75 μm, the results indicated asperity contact for all test condition.

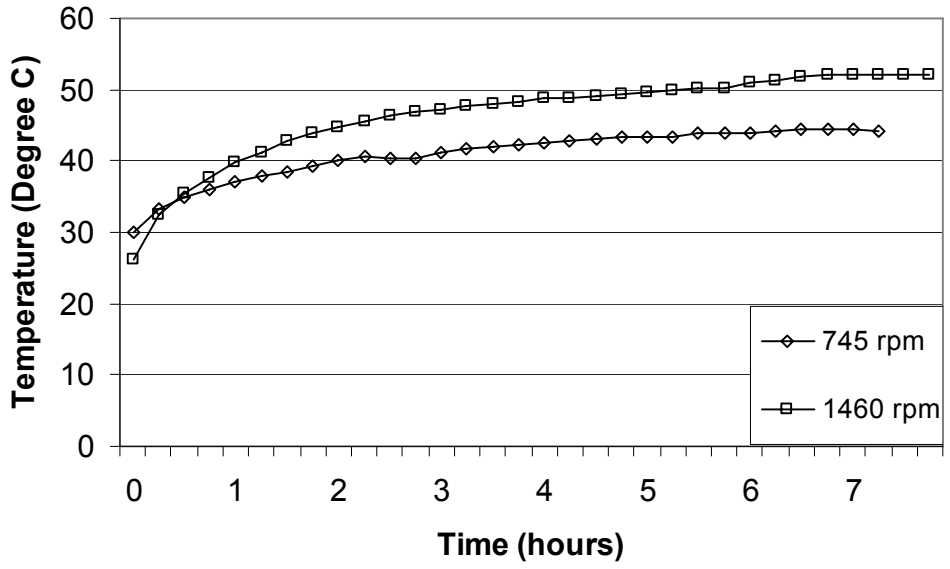

Figure 15 The effect of speed on oil temperature for load of 110 Nm.

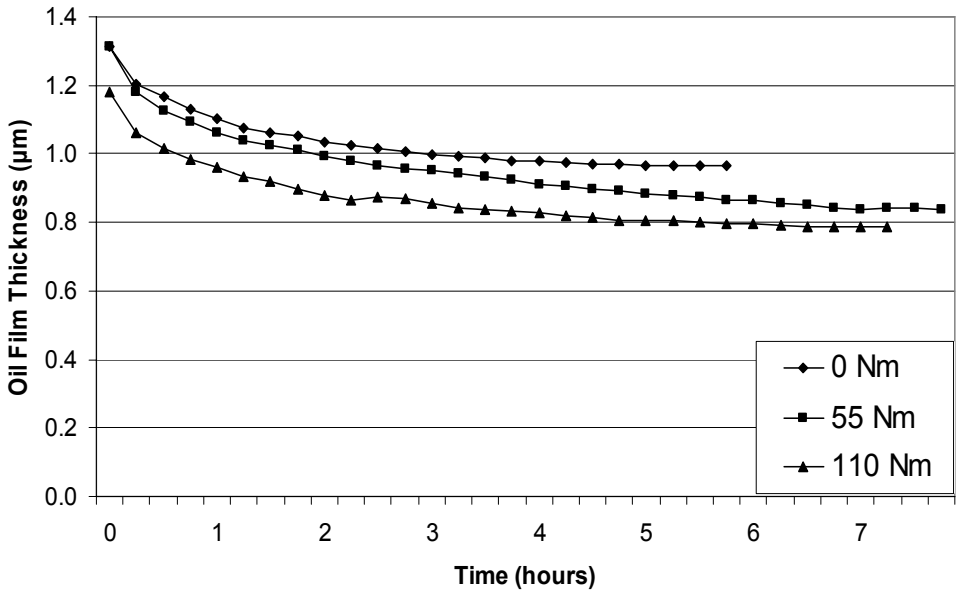

Figure 16 The effect of load on oil film thickness for speed of 745 rpm.

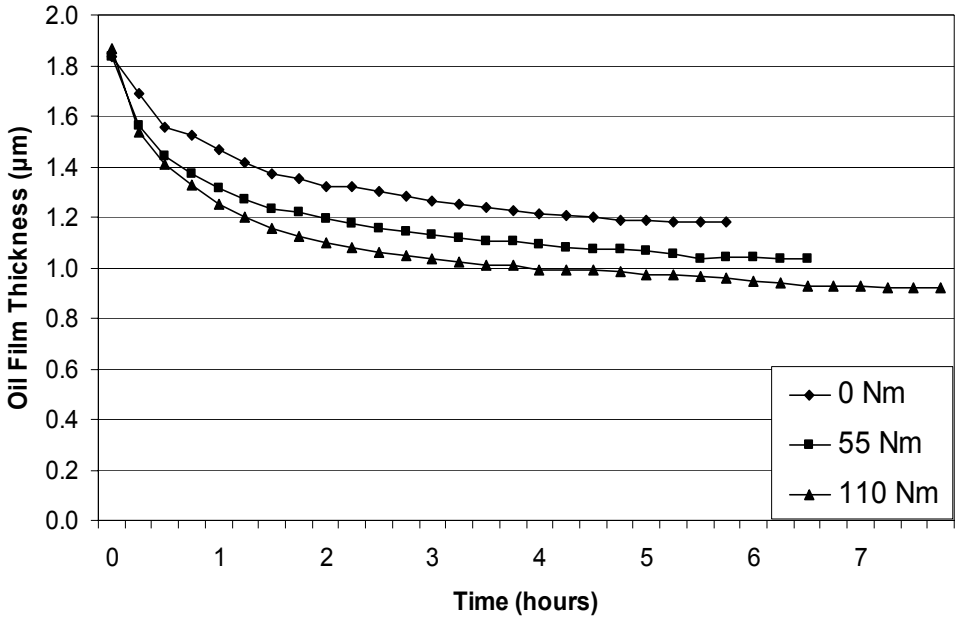

Figure 17 The effect of load on oil film thickness for speed of 1460 rpm.

Possible sources of errors for the oil film thickness calculation include:

- The assumption of constant density, as oil density will change with temperature and affect on oil film thickness.
- The measurement of oil temperatures. It was not possible to measure the oil temperature in the gear mesh due to obvious access problems. Hence, the oil temperatures were taken at the oil bath location as near to the gear mesh as possible. The oil bath temperatures recorded would certainly be lower than the actual oil temperatures.

9.1 Relationship between temperature and AE

The relationship between AE peak amplitude and r.m.s. with load has been detailed [15]. Increasing the load resulted in an increase in AE r.m.s. and peak amplitude. However, the results of AE r.m.s and energy presented thus far were considered unsatisfactory in identifying the defect location. This resulted in yet further tests to explain the discrepancies, particularly as other authors had supported the applicability of these parameters to gear defect detection. These new tests were carried out using the same test set-up, but in this instance the AE r.m.s. and energy data were monitored and recorded continuously while oil temperature in the gearbox was also measured at fifteen minute intervals.

Continuous Acoustic Emission energy and r.m.s values were calculated in real time by the ADC controlling software. The software employed a hardware accelerator so that calculations could be performed in real time. The hardware accelerator takes each value from the ADC and squares it. The results are added into an accumulator for a programmable time interval, based on the user set time constant which in this instance was 100 ms. At the start of the time interval the accumulator is cleared and at the end of the time interval the accumulator value is stored. The r.m.s is then calculated by taking the square root of the sum of the accumulated squared ADC readings. The energy value computed was equivalent to the area under the time waveform and is measured in Atto-Joules. The time interval for acquisition was also set at 100 ms.

These additional tests were run at three load conditions and were started from cold and terminated when the oil temperatures remained stable for one hour. Continuous AE r.m.s. and energy were calculated throughout the period of testing. Equilibrium at the oil temperatures was achieved when the temperature remained within 0.2^0C for the duration of one hour.

A smoothening technique was applied to the continuous AE data using moving average of 255 data points. From figures 18 and 19, it was noted that the AE r.m.s. varied with time as the gear box reached a stabilised temperature. This was observed for both r.m.s and energy values. This implied that depending on what time the AE data was collected for a given speed and load condition, the variation in AE activity r.ms or energy could be as much as 50% for 745 rpm and 125% at 1460 rpm. For these particular tests the point at which the data was captured is highlighted in figures 18 and 19. Thus, the AE signal captured during seeded defect tests were 'snapshots' that are largely influenced by load and oil temperature. As 'snapshots' only provide information at an instance in time, the repeatability of the derived AE parameters will be subjected to considerable variation. The influence of load and oil temperature on AE activity is directly linked to the oil film thickness between the meshing gears. The oil film thickness will influence the rate of wear and asperity deformation, both of which generate the AE activity.

The complications of the effect of oil temperature on AE activity have far reaching consequences, particularly as most of the published work to date have not take cognisance of this effect. The authors of this paper believe it is flawed to compare AE

activity from defect free and/or simulated defect conditions under varying loads without accounting for the influence of oil temperature.

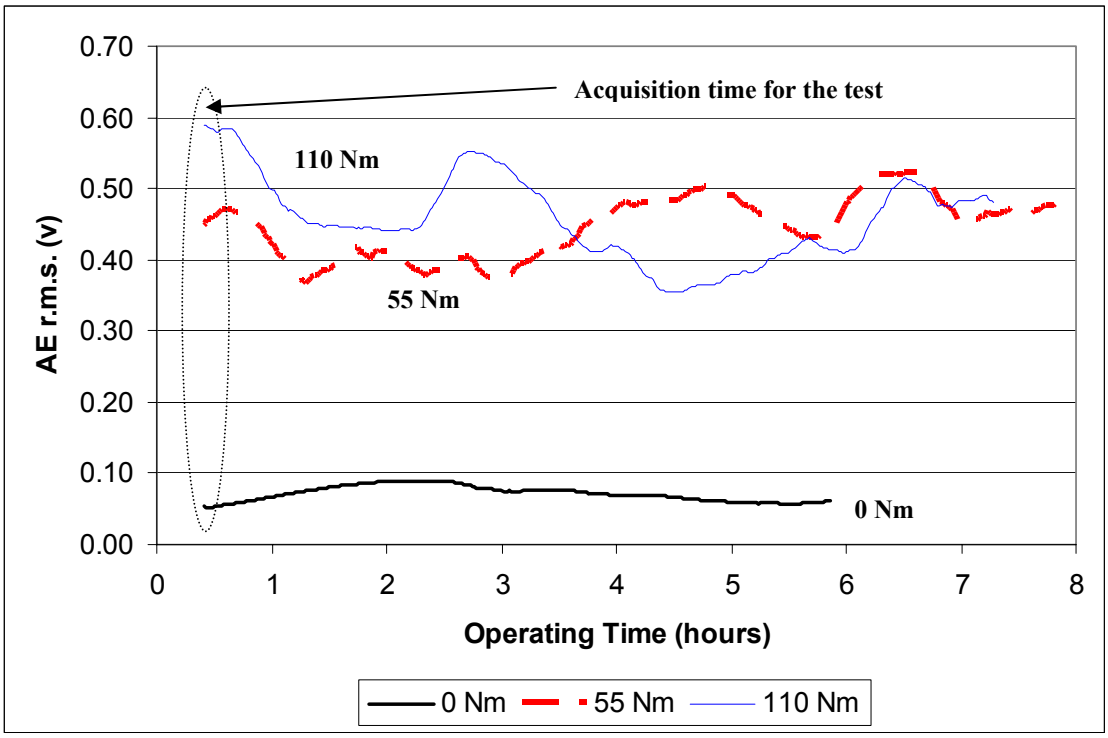

Figure 18 Continuous AE r.m.s values 745 rpm.

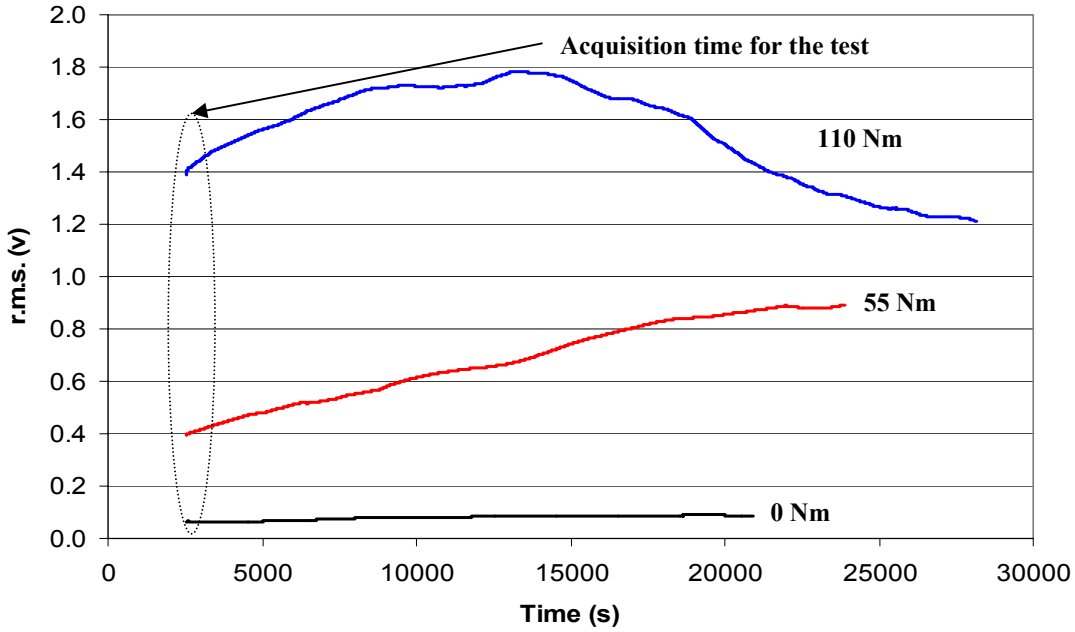

Figure 19 Continuous AE r.m.s values 1460 rpm.

Taking cognisance that AE activity is generated during the sliding of the gears, principally due to asperity contacts [20], the introduction of a seeded defect which removes surface material digresses from the basic source of AE generation. Therefore the authors argue that defect identification of seeded defects of this nature cannot be accomplished with the AE technique. This statement will hold true if seeded defect involved the removal of material from the surface. However, other authors [15, 16, 19] have claimed success and it is argued that the more likely reason for this is as follows: It is highly possible that in the process of material removal from the gear face 'mounds' or 'protrusions' will be formed at the boundaries of the seeded defect, see figure 20. These are created due to the displacement of material from the region of material removal. The authors postulate that it is these 'protrusions' that was responsible for AE activity. However, this activity will only last until the 'protrusions' are flattened during the

operation of the gear, see figure 21. In the later instance, AE will be generated by asperity contacts.

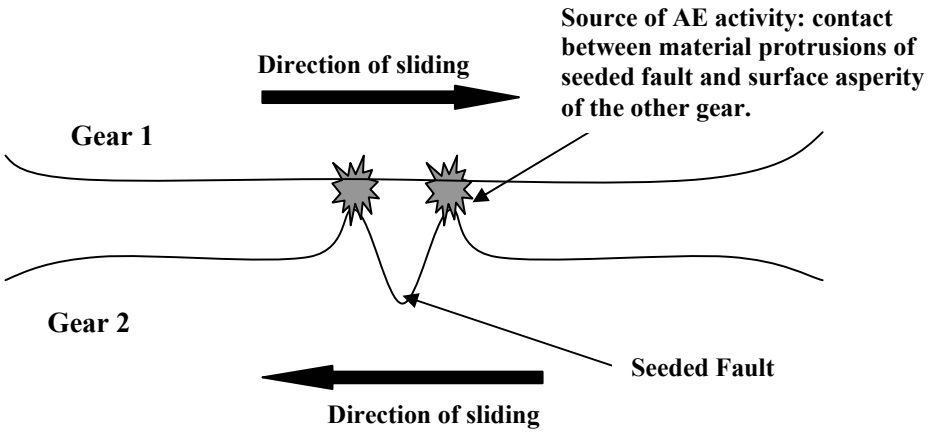

Figure 20 Mounds or Protrusions of the gear surfaces in contact during rotation.

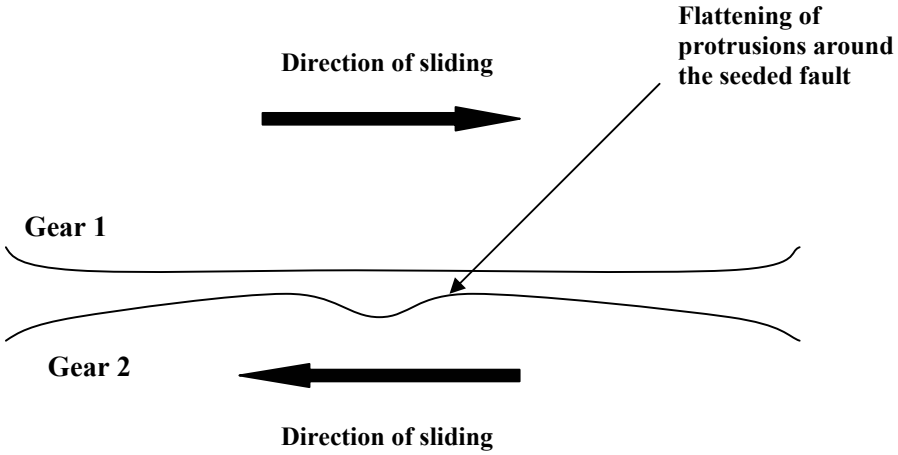

Figure 21 Flattened protrusions of gear surfaces

Whilst researchers [15, 16, 19] have stated that AE indicators such as r.m.s. and energy increased with increasing load and speed, none have taken cognisance of the effect of temperature on AE activity. Clearly measuring the load and speed will cause a change in lubricant temperature. The authors believe that the lubricant temperature is the dominant factor in the AE generation and the load or speed is a secondary factor of the oil temperature. This has far reaching consequences as it implies that whilst other researchers have stipulated the effect of load/speed on AE activity, the time of data acquisition, in effect the temperature of the lubricant, will determine what values of r.m.s. are obtained. If as observed in this paper, the AE parameters continually change for several hours, the data presented by other researchers are subjected to variation caused by environmental conditions. This implies that even if attempts were undertaken to collect AE data at specified times, the effect of ambient temperature, which will influence the temperature at which the data is collected, could present inconsistencies or repeatability issues. Developing AE as a robust diagnosis tool without taking cognisance of the temperature influence will not be robust. To prove this postulation, the authors undertook an additional test.

10. Constant Temperature Tests

The three main factors affecting the AE signal in these experiments are namely; speed of rotation, applied torque (load) and the oil temperature. In order to further examine the speed and load effect on AE signal for this back-to-back gearbox arrangement, constant

temperature tests were performed. Since the oil temperatures were kept constant, the oil viscosity and film thickness will remain constant during the experiment.

The gearbox was run at 745 rpm with a load of 220 Nm for 5 hours at which time the oil temperature stabilised at 42.7^0C. The gearbox was brought to a stop and adjusted to no-load condition. The gearbox was re-started and run for 10 minutes whilst continuous AE data in the form of r.m.s and energy was recorded. The gearbox was again brought to a stop and adjusted to the next load condition. Every load condition was run for a 10-minute interval while the continuous AE r.m.s. and energy data were taken. The time taken to strip the rig and set the new torque level was approximately three minutes. During this period the acquisition system was paused. A total of 5 load conditions; 0, 55, 110, 183 and 220 Nm, were tested. In these tests, the average oil temperature was at 42.4^0C with a maximum temperature difference of 1.8^0C to minimise the temperature effect.

At the rotational speed of 745 rpm, the continuous AE r.m.s. values were plotted for the 5 loading conditions and presented in figure 22. It was observed that the AE r.m.s remained rather constant at 0.58 volts with increasing loads. For the 1460 rpm test condition, the same test procedures were employed, the oil temperature stabilised at 51.8^0C. The mean oil temperature was kept at 50.8^0C with a maximum temperature difference of 3.5^0C to ensure constant temperature condition. The AE r.m.s. was plotted against the five loading conditions, see figure 23. Similar trends were observed when compared to the lower running speed condition. With increasing load, the AE r.m.s remained constant at 1.2

volts. From the above results, it can be concluded that at constant oil temperature, the applied load on the gear system had negligible effect on AE r.m.s. On the other hand, speed had a more significant effect on the AE indicators. By doubling the rotational speed from 745 rpm to 1460 rpm, the AE r.m.s increased from 0.58 to 1.2 volts by a factor of 2. Between the two rotational speeds, there was a temperature difference of 8.4^0C.

Boness et al [20] showed that AE r.m.s increased with decreasing viscosity. Hence, for this experiment, the increase in the AE parameters at 1460 rpm was partially due to the higher oil temperature at the higher rotational speed. This will be the topic of future research by the authors.

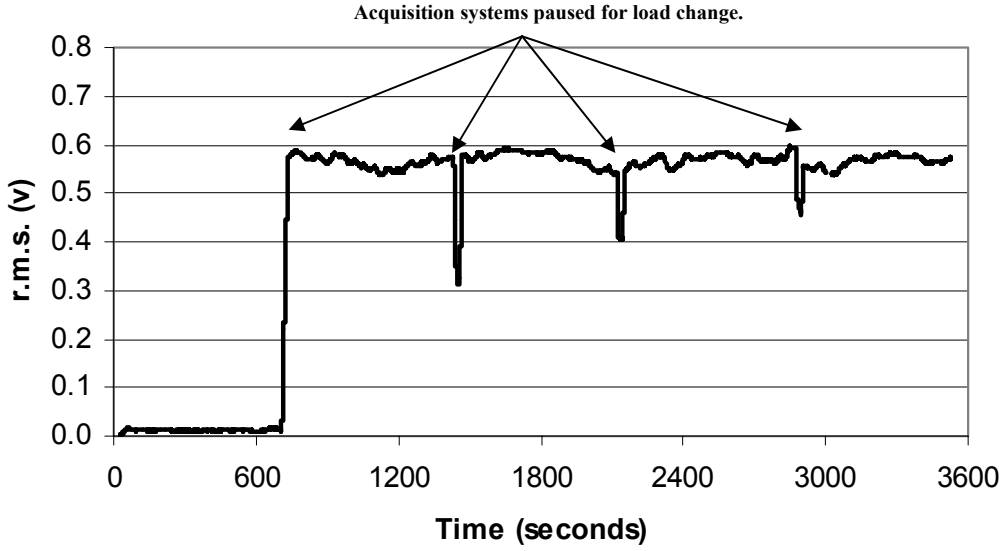

Figure 22 AE r.m.s. remained constant with increased load at 745 rpm

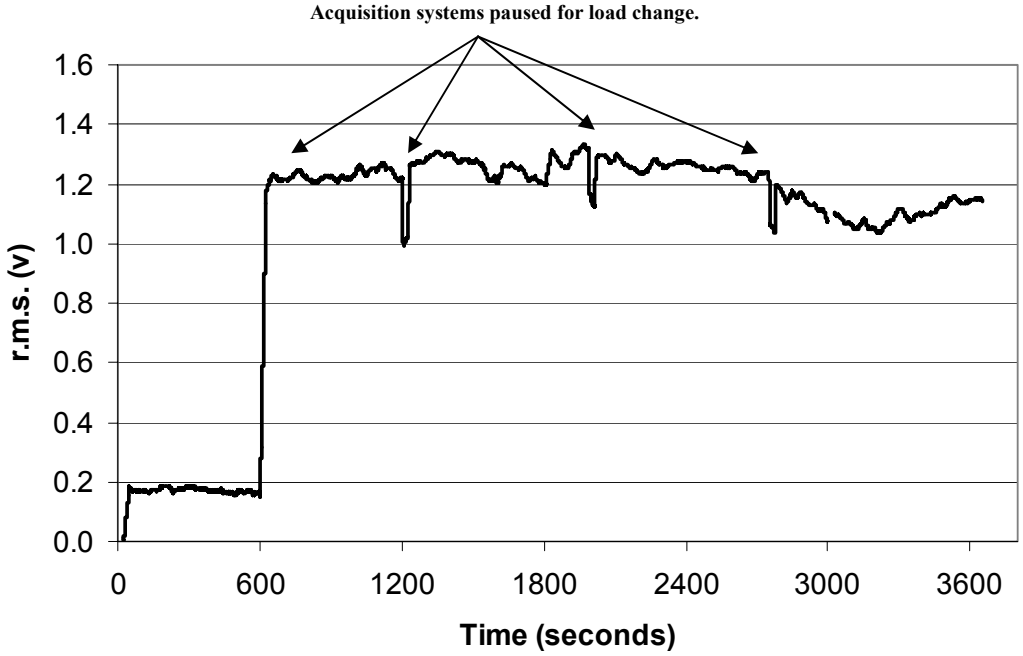

Figure 23 AE r.m.s. remained constant with increased load at 1460 rpm

11 AE Source Mechanisms

From the observations presented thus far two possible sources of AE were identified; tooth resonance and asperity contacts.

11.1 Tooth resonance

Estimation of the tooth resonance frequency was accomplished by modelling the gear tooth as a cantilever beam and spring mass systems. Using the gear tooth geometries, loading boundary conditions and the assumption that the load is transmitted through the pitch-line, the tooth resonance frequency was calculated at 75kHz. This eliminated gear tooth resonance as a source of AE activity in the gear mesh.

11.2 Friction and asperity contacts

During the gear mesh; sliding, rolling or a combination of both will occur. As the gear teeth surfaces are limited to manufacturing capabilities (approximately 0.4μm) asperity contacts will occur during meshing on almost all gears, particularly as the calculated oil film thickness in this instance is less than the composite roughness.

During gear experiments, Smith [23] noted transient shock pulses during gear mesh at the gear mesh frequency. It was concluded that these shocks were attributed to asperity contact. Whilst a single asperity model was presented as the probable cause of the shocks, the likelihood of such scenario in practice is limited, multiple contacts will be present. However, it was shown that based on a asperity width of 5μm and sliding and rolling velocities of the order of 500mm/s, the raise time for such a transient event was 10μs. It must be noted that the sensors employed by Smith had a natural frequency of 50 kHz and is outside the range of AE.

The relationship between sliding and rolling friction has been investigated [22]. It was shown that whilst the rolling friction traction is independent of load the sliding friction traction is influenced by the lubricant viscosity and load. Furthermore, it was shown that increasing rolling speed resulted in a reduction of friction traction for a fixed load and lubricant viscosity. Following observations presented in this paper of relatively constant r.m.s. values at a fixed speed and temperature irrespective of load, some resemblance to the phenomena of rolling friction, and elastohydrodynamic lubrication, as detailed by Dowson et al is evident.

Studies in tribology are significant to the work presented. Boness et al [20] studied the oil viscosity effects on AE and wear in lubricated sliding contacts. Several observations were noted including an increase in AE r.m.s with decreasing viscosity and increased rotational speed, but more importantly, the source of AE under lubricated sliding conditions was attributed to asperity contact. In relating AE to sliding friction Dornfeld [24] et al have shown the high sensitivity of AE to sliding speed and applied load. It was noted that the basic mechanism for AE generation was the elastic deformation of the material at asperity contacts. This deformation was accented or mated by increased rates (sliding speed), contact forces and lubrication. The range of surface finish for the materials investigated was from 1 to 4μm; comparable with the gears tested in this study.

All the above comments provided strong evidence to suggest that the source of AE during gear mesh is attributed to asperity contact. The authors are currently investigating this phenomenon in more detail and results of the study will be subject to future publication.

12. Conclusion

The main element contributing to the change in vibration level is the stiffness of the operating gear system. Hence, as long as the defect is able to alter the stiffness of the system, it will be detected by the accelerometer, as observed in the experiments reported. This is in contrast to the AE technique which was excited by asperity contacts.

The general relationships between monitoring parameters (such as vibration and AE indicators) and the gearbox operating conditions (such as load, speed and oil film

thickness) have been established in this experiment. It is important to note that various indicators within a monitoring technique must be used simultaneously in order to establish and explain the phenomena observed. The most ideal situation is to use various techniques to monitor the gearbox health status at the same time. This paper has demonstrated that gear defect detection with AE is fraught with difficulties. Seeded defect identification with AE r.m.s. and energy were not satisfactory. The influence of oil temperature on AE activity has been presented as the primary reason for this limitation. It is concluded that the source of AE mechanism that produced the gear mesh bursts was from asperities contact. It is postulated that the variation in amplitude of each AE transient burst at the mesh, as evident in figures 5 to 7, is attributed to the changing nature of the asperity contact with time, particularly as the individual teeth involved in each mesh are not identical at each mesh due to the difference in number of teeth on each wheel.

Finally, the constant temperature tests have revealed far reaching consequences which may alter the approach of applying AE technique to gear fault diagnosis and monitoring. Furthermore, it may offer tribologists a means of assessing the effectiveness of a lubricant under a range of operating condition.

13. References

1. Miller, R.K. and McIntire, P. Acoustic Emission Testing, Volume 5, 2nd ed., Non-destructive Testing Handbook. Ed., American Society for Non-destructive Testing, pp 275-310, 1987.

2. Mba, D. and Bannister, R.H. Condition monitoring of low-speed rotating machinery using stress waves: Part1 and Part 2. Proc Inst Mech Engrs. 213(3), Part E, 153-185. 1999.

3. Morhain, A. and Mba, D. Bearing defect diagnosis and acoustic emission Journal of Engineering Tribology, I Mech E, Vol 217, No. 4, Part J, p 257-272, 2003. ISSN 1350-6501Mba, D. (2002).

4. Mba, D. Applicability of acoustic emissions to monitoring the mechanical integrity of bolted structures in low speed rotating machinery: case study. NDT and E International. 35(5), 293-300. 2002.

5. Mba, D., Cooke, A., Roby, D. and Hewitt, G. Detection of shaft-seal rubbing in large-scale power generation turbines with Acoustic Emissions; Case study. Journal of Power and Energy - Part A, I Mech E, Vol 218, No. 2, Part A, p 71-82, March 2004. ISSN 0957-6509.

6. Toutountzakis, T. and Mba, D. Observation of Acoustic Emission Activity During Gear Defect Diagnosis. NDT and E International. 36(7), 471-477. 2003.

7. Bruzelius, K. and Mba, D. An initial investigation on the potential applicability of Acoustic Emission to rail track fault detection. NDT & E International, 37(7), 507-516. 2004.

8. Hall, L.D. and Mba, D. Diagnosis of continuous rotor–stator rubbing in large scale turbine units using acoustic emissions, Ultrasonics, 41(9), 765-773. 2004.

9. Hall, L.D. and Mba, D. Acoustic emissions diagnosis of rotor-stator rubs using the KS statistic, Mechanical Systems and Signal Processing, 18(4), 849-868. 2004.

10. Mba, D and Jamaludin, N. Monitoring extremely slow rolling element bearings: Part I and II, NDT and E International, 35(60), 349-366, 2002.

11. Gadd, P. and Mitchell, P.J. Condition monitoring of helicopter gearboxes using automatic vibration analysis techniques. AGARD CP 369. Gears and power transmission system for helicopter turboprops. 29/1 – 29/10.1984.

12. Leblanc, J.F.A., Dube, J.R.F. and Devereux, B. Helicopter gearbox vibration analysis in the Canadian Forces-applications and lessons. *1st International Conference, Gearbox noise and vibration.* IMechE, Cambridge, UK. C404/023, pp 173 -177. 1990.

13. Cameron, B.G. and Stuckey, M.J. A review of transmission vibration monitoring at Westland Helicopter Ltd. 20Th European Rotorcraft Forum. Paper 116. pp 116/1 – 116/16. 1994.

14. Drosjack, M.J. and Houser D.R. An experimental and theoretical study of the effect of simulated pitch line pitting on the vibration of a geared system. ASME Publication Report 77-DET-123, 1977.

15. Tandon, N. and Mata, S. Detection of Defects in Gears by Acoustic Emission Measurements, Journal of Acoustic Emission. **Vol. 17**, Issue 1-2, 23-27, 1999.

16. Singh, A., Houser, D. R., and Vijayakar, S. Early Detection of Gear Pitting, Power Transmission and Gearing Conference, ASME. **DE-Vol. 88**, 673-678, 1996.

17. Singh, A., Houser, D. R., and Vijayakar, S. Detecting Gear Tooth Breakage Using Acoustic Emission: A Feasibility and Sensor Placement Study, Journal of Mechanical Design. **Vol. 121**, 587-593, 1999.

18. Sentoku, H. AE in Tooth Surface Failure Process of Spur Gears, Journal of Acoustic Emission. **Vol. 16**, Issue 1-4, S19-S24, 1998.

19. Siores, E. and Negro, A.A. Condition Monitoring of a Gear Box Using Acoustic Emission Testing, Material Evaluation. 183-187, 1997.

20. Boness, R.J. and McBride, S.L. Adhesive and abrasive wear studies using acoustic emission techniques. Wear. **Vol. 149**, 41-53, 1991.

21. Smith, J.D. Gear noise and vibration, 1st ed. New York: Marcel Dekker In cooperation, 1999.

22. Dowson, D. and Higginson, G.R. Elasto-hydrodynamic Lubrication. 1st ed. Oxford: Pergamon Press, 1977.

23. Smith, J.D. A new diagnostic technique for asperity contact. Tribology International. **Vol. 26**, pp 25-27. 1993.

24. Dornfeld, D. and Handy, C. Slip detection using acoustic emission signal analysis. *IEEE International Conference on Robotics and Automation.* **Vol. 4**, pp 1868 - 1875. 1987.

https://dspace.org/

Identification of the acoustic emission source during a comparative study on diagnosis of a spur gearbox

Tan, Chee Keong; Mba, David

2005-05-01T00:00:00Z
Elsevier Science B.V., Amsterdam.
http://dx.doi.org/10.1016/j.triboint.2004.10.007
Chee Keong Tan and David Mba, Identification of the acoustic emission source during a comparative study on diagnosis of a spur gearbox, Tribology International, Volume 38, Issue 5, May 2005, Pages 469-480.

Downloaded from a DSpace repository. https://dspace.org/